

Automatic high resolution measurement set-up for calibrating precise line scales

Klobucar, R.^{a,*}, Acko, B.^a

^aFaculty of mechanical engineering, University of Maribor, Maribor, Slovenia

ABSTRACT

This paper presents a high resolution measurement set-up developed for calibrating precise line scales with measurement uncertainty of less than 0.1 μm over a total length of 500 mm. The system integrates a numerically controlled multi-axis stage, a laser interferometer, and a vision system for detecting line position. The measurement and the analysis processes are completely automated in order to minimize manual labour during the calibration process, but also increase the calibration accuracy. Increasing calibration accuracy leads up to better quality of industrial measurements which is required by modern precision industry. When designing this set-up, special attention was paid to the alignment of the measurement object in the measurement direction, considering the focus of the camera. The aim of this alignment was to reduce Abbe errors in 2 axes to negligible level. In addition, all uncertainty contributions have been determined and evaluated by performing extended experiments in specific measurement conditions. These contributions are presented in the uncertainty budget. The metrological capabilities of the presented measurement set-up were verified by some practical test measurements. Selected results of these measurements are presented in the article. This set-up will primarily improve a standard base for calibration of optical measuring devices. The use of the optical standards in the industry is constantly growing. Indirect users of the results of this research will be all manufacturers of precise products such as automotive and other industries.

© 2017 PEI, University of Maribor. All rights reserved.

ARTICLE INFO

Keywords:

Measurement
Line scales
High resolution measurements
Measurement uncertainty

*Corresponding author:

rok.klobucar@um.si
(Klobucar, R.)

Article history:

Received 15 September 2016

Revised 27 February 2017

Accepted 1 March 2017

1. Introduction

Line scales and grid plates are most common measurement standards for assuring traceability of optical measuring equipment, such as microscopes, profile projectors and digital “vision” systems. They are widely used in industry and research laboratories as calibration standards [8]. Line scales are important material standards of length, used for accurate positioning or measurement in one, two or three dimensions [1].

Industry is demanding more and more rapid and accurate dimensional measurements on diverse mechanical parts. In recent years, optical coordinate measuring machines (CMMs) having made substantial progress and are now often used for such applications. Especially CMMs equipped with imaging capabilities are frequently used for fast, non-contact measurements. Strong competition among manufacturers of such instruments and the demand for sub-micron accuracy has led to standardised tests, which are aimed for comparing and validating instrument performance [2]. Calibration, verification and also error correction of

optical CMMs are mainly based on measurements using reference line scales or two-dimensional grid plates [3].

There are very many commercially available line scales made of different materials (steel, brass, invar, glass, quartz, zerodur). They can vary in length from below 1 mm to more than 1 m, and have resolutions (pitch) from below 10 nm to 1 cm. They can be calibrated by using different measurement set-ups, depending on their length and precision. Set-ups for calibrating high-precision line scales normally involve a microscope with an optical sensor for capturing and analysing the image of a line marker and a laser interferometer as a traceable measurement standard [4-6].

This paper introduces a measuring system developed for calibrating line scales with measurement uncertainty of less than 10 nm over a total length of 500 mm. The system integrates a numerically controlled multi-axis stage, a laser interferometer, and a vision system for detecting line position. With this measurement set-up, Abbe errors can be reduced to negligible levels. Abbe error occurs when the measurement point of interest is spatially separated laterally from the actual measuring scale location (reference line or axis of measurement), and when angular error motions exist in the positioning system. Abbe error causes measured displacement to appear longer or shorter than the true displacement, depending on the direction of angular motion. Spatial separation between the measured point and reference line is known as an Abbe offset [7].

Since it is possible to put optical components very close to each other, the air dead path error of the laser interferometer is also negligible. Software for detecting the middle of the lines is based on earlier design from 2009 [9]. In order to improve performance and to achieve better uncertainty, the software was improved and automatized, mechanics and optics have been redesigned and several uncertainty components better characterized. This facility will replace the old measurement facility that is manually operated. A model for evaluating uncertainty and the uncertainty budget for the demonstrated measuring system is presented in the paper.

2. Measurement system

2.1 Numerically controlled multi-axis stage

Numerically controlled multi-axis stage was designed and manufactured by Newport-micro controle [10] for the Laboratory for Production Measurement (LTM), University of Maribor, Slovenia. It is shown in Fig. 1, while its schematic diagram is shown in Fig. 2. The measuring system designed by the LTM is intended to perform 2D measurements on various objects, which will be fixed on a measuring table. This research is focused in 1D measurements. Newport's solution is based on a HybrYX-G5 stage featuring a ceramic carriage which freely slides in X and Y axes on a precision lapped granite reference plate, using proprietary pressure-vacuum air bearing design. The carriage is guided along Y axis by a rigid ceramic beam. The beam is supported and guided at each end with the ball bearing carriages of X axis. Both X and Y axes are motorized with linear actuators and include linear glass encoders. Both linear scale glass encoders are LIDA403 made by Heidenhain, length 440 mm for X axis and length 1250 mm for Y axis. This positioning system is equipped with the optional Z-Tip-Tilt and Theta stage. It is motorized by precision actuators equipped with miniature DC servo motors. The position system is built on a heavy granite table, which features a precision reference plane for the air bearing carriage. In addition, the granite structure includes a granite gantry allowing the fixation of a vertical motorized translation stage, which accommodates the measuring sensor, depending on an application. Two rails mounted on the gantry equipped with sliding carriages provide manual rough positioning capability. The granite structure is set on a heavy welded frame equipped with ND40 passive isolators. The position system has one XPS motion controller including dedicated drivers for the five DC motors and the three linear motors.

The X axis is dual axis composed of X1 and X2 actuators mounted on the flanks at both ends of the granite table. X1 and X2 carriages move the ceramic beam of the Y axes. The X axis travel

range is ± 175 mm. It has a linear encoder with 5 nm resolution. The maximal speed is 300 mm/s., while the repeatability is 500 nm.

The Y axis is a horizontal translation stage using air bearing technology and linear motor. The guiding beam of Y axes sub-assembly is attached to the carriages of the X1 and X2 short travel translation actuators. The guideways involve two parts: a large ceramic carriage and a Y-axis guide ceramic L-shape beam. The ceramic carriage freely slides in X and Y axes using pressure-vacuum air bearing design. The reference planes for the air bearing carriage are the precision lapped surface of the granite table and the vertical slide of the Y rigid ceramic beam. The Y axis travel range is ± 500 mm. It contains a linear encoder with 5 nm resolution. Maximum speed is 600 mm/s., while the repeatability is 100 nm.

The ZTT Theta stage is mounted on the air bearing carriage; it is equipped at the top with the measuring platform, which allows installing measured objects. All axes are driven by the high precision motorized linear actuators. Three actuators are set in upright position with a travel range of 10 mm. One actuator is set horizontally to achieve the theta Z movement with a travel range of $\pm 1^\circ$. All four actuators are equipped with a miniature DC motor made by Fulhaber.

Z axis is a vertical motorized translation stage on the middle carrier. It is a Newport catalogue stage reference M-IMS100V. The Z axis travel range is 100 mm, the minimum incremental motion is $0.3 \mu\text{m}$, the encoder resolution is $0.1 \mu\text{m}$, the maximum speed is 20 mm/s, while the repeatability is $\pm 0.5 \mu\text{m}$.

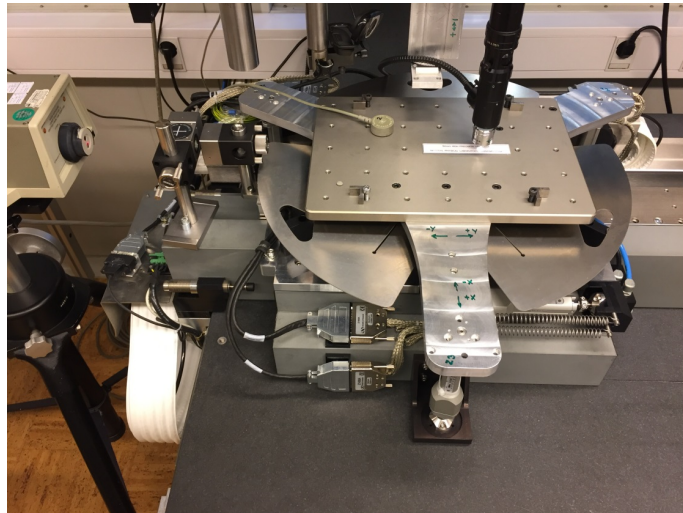


Fig. 1 Measurement set-up for calibrating line scales

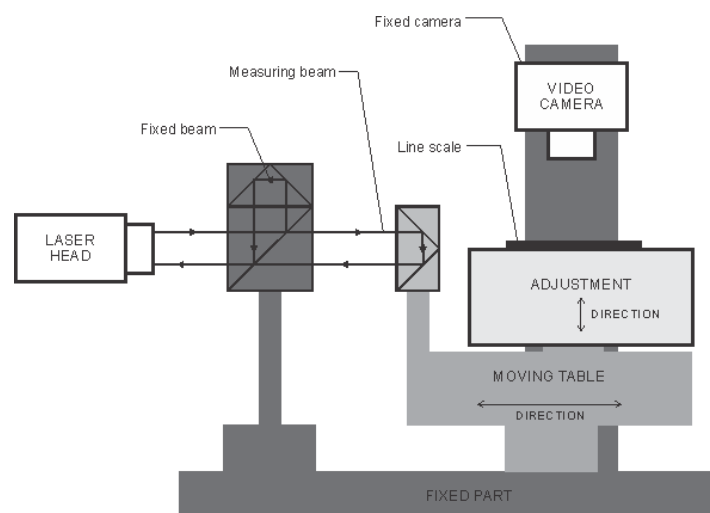


Fig. 2 Schematic diagram of measurement set-up for calibrating line scales

2.2 Laser interferometer

Laser interferometer position measurement systems provide very precise position or distance information. Our system consists of a laser head HP 5528A, Agilent module 55292A, and a variety of optical components and accessories such as material sensors and air sensor. The basic system measures linear displacement. The system uses the wavelength of light from a low-power helium-neon laser as a length standard. We normally set the resolution of the laser interferometer to 10 nm. Special mounting elements were constructed for the optics used for calibration. A schematic diagram of the laser interferometer and the position of the optics are shown in Fig. 2. The position of the optical elements and the moving parts are set in such way, that the measured object axis is set in the line with the centre of the laser linear retroreflector. It allows the Abbe errors to be reduced to negligible levels even for the most demanding dimensional metrology tasks [11]. The linear interferometer is fixed on the fixed part of the stage, while the retroreflector is placed on the moving table in the horizontal direction. Only the measured object is placed on the moving table that can move in the vertical direction.

2.3 Vision system for detecting line position

The vision system for detecting line position consists of a zoom microscope and a CMOS digital camera. The camera is connected to the computer via USB 3.0 port. The CMOS camera gets the images of the line scale and sends them to the computer software. The software analyses the images and determines the middle of the line in the measured window as shown in Fig. 3, which is defined by the operator. The software calculates the distance in pixels from the reference position, which is marked with the blue line, to the middle of the measured line that is marked with the red line. The image positioning screen with the measurement window, reference and measured line is presented in Fig. 3. The CMOS digital camera takes 15 monochrome images per second in resolution 2592×1944 pixels. The software analyses the images in real time. The distance calculated in pixels is transformed into micrometers [12]. The software for calculation the distance between lines is more detailed presented by the authors in paper [9].

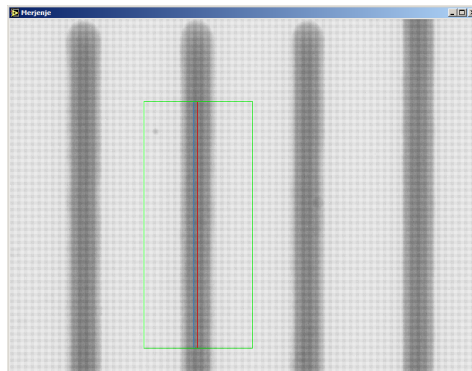


Fig. 3 Screen image of the vision system for detecting line position

2.4 Measurement procedure

Line scales are material measures made of glass, steel or other material, on which dimensions are marked with line marks. Since the materials have quite different temperature expansion coefficients, which are in many cases not exactly known, they are stabilized before calibration in the climatic room at 20 °C for 24 hours. The measurement system must be adjusted and initialized before the measurement. The line scale should be positioned under the camera by moving the measurement table. The measuring system, laser interferometer, vision system for detecting line position and line scale should be adjusted according to the measuring direction, which is defined by the movement of the horizontal direction of the table. The line scale should be fixed on the adjustment table under the camera. The camera is fixed. It is adjusted in such a way, that the focus of the camera intersects the centre of the laser linear retroreflector. The camera is focused on the lines of the line scale by moving the adjustment table (ZTT Theta stage)

in the vertical direction. With this procedure, the line scale axis, the images of the lines and the centre of the laser linear retroreflector with the laser beam are positioned in the measuring direction. The image processing software should be initialized [9]. With the improved software, connection to the numerically controlled multi-axis stage and connection to the laser head, automatic measurements of distances are possible. The measurement goal is to measure distances between the reference line and the chosen measuring lines on the line scale automatically. Measured data are saved into the file where they are ready for further processing.

2.5 Principle for minimising Abbe error

In respect to the movement parts of the measuring system, the system can be divided into three different parts. The first part is the fixed part and it includes the laser head, the linear interferometer and the USB 3.0 camera. The second part is the moving part in the horizontal direction and it includes the linear retroreflector, the moving table and the measured object. The third part is the moving part in the vertical direction and it includes the moving table and the measured object. The third part is used only for adjusting the line scale in respect to the measuring object direction. The camera is in the fixed distance, so that the focus of the camera is on the top of the moving table. This means that the theoretical measured lines that could be on the top of the table, are in the focus of the camera and simultaneously with the laser optics. Only the moving table with the line scale could be moved in the vertical direction. This procedure allows us moving the lines of the line scale into the focus of the camera and in the same time into the centre of the laser optics. With this procedure, the minimum Abbe error can be achieved.

One of the most important sources of error in dimensional measurement is Abbe error. Abbe error consists of an Abbe offset and a small angular variation due to pitch and yaw of the stage that moves the measuring table with the measured object and the linear retroreflector. This component is caused by the measuring table inclination along the measurement path (Y axis). The best available tool for analysing angular error is a laser interferometer. Pitch and yaw measurements were made by making angular measurements at multiple points along the linear travel path in the Y axis as shown in Fig. 4. The angles of the measuring table were measured by using angular interferometer optics. The greatest Abbe errors were evaluated by analysing extreme angular deviations.

For pitch (Fig. 4), the greatest angle differences along the measurement path of 500 mm was 7 $\mu\text{m}/\text{m}$. The maximum offset of the laser reflector of 3 mm in the Z direction was estimated. Therefore the expected error interval for pitch is:

$$I = 7 \text{ nm/mm} \cdot 3 \text{ mm} = 21 \text{ nm} \quad (1)$$

Standard uncertainty at supposed rectangular distribution for the Abbe error for pitch is:

$$u_{zy}(e_a) = \frac{21 \text{ nm}}{\sqrt{3}} = 12 \text{ nm} \quad (2)$$

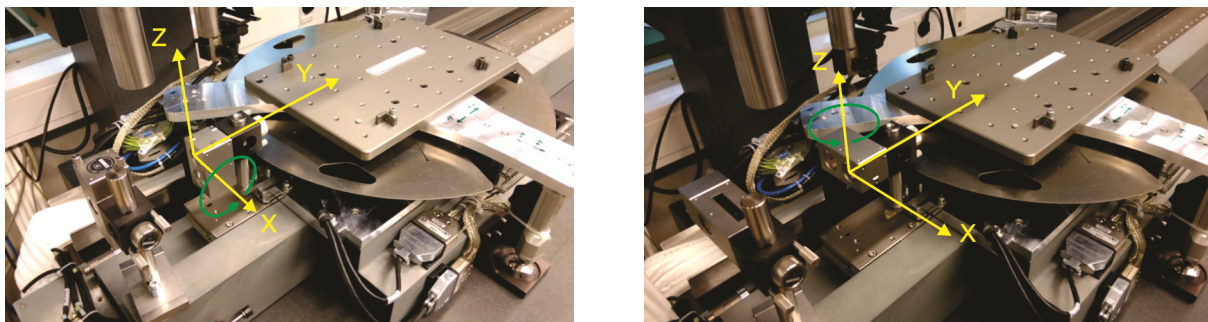


Fig. 4 Pitch and yaw measurements of the stage in Y direction

For yaw (Fig. 4), the greatest angle differences along the measurement path of 500 mm was 10 $\mu\text{m}/\text{m}$. The maximum offset of the laser reflector of 1 mm in the X direction was estimated. Therefore the expected error interval for the yaw is:

$$I = 10 \text{ nm}/\text{mm} \cdot 1 \text{ mm} = 10 \text{ nm} \quad (3)$$

Standard uncertainty at supposed rectangular distribution for the Abbe error for the yaw is:

$$u_{xy}(e_a) = \frac{10 \text{ nm}}{\sqrt{3}} = 5.8 \text{ nm} \quad (4)$$

Total standard uncertainty due to Abbe error $u(e_a)$ is:

$$u(e_a) = \sqrt{u_{zy}^2(e_a) + u_{xy}^2(e_a)} = 13 \text{ nm} \quad (5)$$

3. Uncertainty of measurement

3.1 Mathematical model of measurement

The measured value in the calibration of a line scale is a deviation from a nominal distance between two line centres. The distance between two lines is calculated as a sum of laser interferometer indication and vision system for detecting line position indication. The vision system for detecting line position measures the distance between the measurement point (scale mark) and the reference line. Deviation e (measurement result) is given by the expression:

$$e = (L_{LI} + L_V - L_{LIref}) \cdot (1 + \alpha_m \cdot \theta_m) - N + e_{\cos} + e_{mp} + e_{ms} + e_a \quad (6)$$

where:

e	deviation (measurement result) at 20 °C
L_{LI}	corrected length shown by laser interferometer
L_V	distance between the measurement point (scale mark) and reference line in the image window
L_{LIref}	indication on the laser in the reference (origin) point
α_m	linear temperature expansion coefficient of the scale
θ_m	temperature deviation of the scale from 20 °C
N	nominal value (without uncertainty)
e_{\cos}	cosine error of measurement (supposed to be 0)
e_{mp}	dead path error
e_{ms}	random error caused by uncontrolled mechanical changes
e_a	error caused by the measuring table inclination

3.2 Standard uncertainty

For uncorrelated input quantities the square of the standard uncertainty associated with the output estimate y is given by equation (7) [12]:

$$u^2(y) = \sum_{i=1}^N u_i^2(y) \quad (7)$$

The quantity $u_i(y)$ ($i = 1, 2, \dots, N$) is the contribution to the standard uncertainty associated with the output estimate y resulting from the standard uncertainty associated with input estimate x_i [12]:

$$u_i(y) = c_i \cdot u(x_i) \quad (8)$$

where c_i is the sensitivity coefficient associated with the input estimate x_i , i.e. the partial derivative of the model function f with respect to X_i , evaluated at the input estimates x_i [12].

$$c_i = \frac{\partial f}{\partial x_i} = \frac{\partial f}{\partial X_i} \Big|_{x_1=x_1, \dots, x_N=x_N} \quad (9)$$

Table 1 Uncertainty budget for calibration of line scales

Value X_i	Estimated value	Standard Uncertainty	Distribution	Sensitivity coefficient	Uncertainty contribution
L_{Li}	0 mm	13 nm + $0,2 \cdot 10^{-6} \cdot L$	normal	1	13 nm + $2,5 \cdot 10^{-7} \cdot L$
L_V	<5 μm	25 nm	normal	1	25 nm
$L_{Li\text{ref}}$	0 mm	9 nm	normal	-1	9 nm
α_m	$10^{-5} \text{ } ^\circ\text{C}^{-1}$	$1,15 \cdot 10^{-6} \text{ } ^\circ\text{C}^{-1}$	rectangular	$0,05 \text{ } ^\circ\text{C} \cdot L$	$0,06 \cdot 10^{-6} \cdot L$
θ_m	$0 \text{ } ^\circ\text{C}$	$0,05 \text{ } ^\circ\text{C}$	normal	$10^{-5} \text{ } ^\circ\text{C}^{-1} \cdot L$	$0,05 \cdot 10^{-5} \cdot L$
e_{\cos}	0	0 nm	normal	1	0 nm
e_{mp}	0	9 nm	rectangular	1	9 nm
e_{ms}	0	30 nm	normal	1	30 nm
e_a	0	13 nm	rectangular	1	13 nm
				Total:	$\sqrt{(45 \text{ nm})^2 + (5,6 \cdot 10^{-7} \cdot L)^2}$

3.3 Expanded uncertainty

Combined standard uncertainty, calculated from the uncertainty budget, is:

$$u = \sqrt{(45 \text{ nm})^2 + (5,6 \cdot 10^{-7} \cdot L)^2} \quad (10)$$

The expanded uncertainty for the coverage factor $k = 2$ is then:

$$U = \sqrt{(90 \text{ nm})^2 + (1,1 \cdot 10^{-6} \cdot L)^2} \quad (11)$$

3.4 Experimental results

The measurement accuracy of the numerically controlled multi-axis stage was verified with the laser interferometer [9] in Y direction over the distance (0 to 500) mm by twenty repeated measurements in eleven positions. The absolute difference between the reference value shown by the laser interferometer and the encoder value in the Y axis of the measuring system is shown in Fig. 5.

Experimental standard deviation that reflects random influences is shown in the diagram in Fig. 6. Random influences are caused by the multi-axis stage instability, vibrations and random changes of environmental conditions. Presented standard deviations were used in uncertainty budget of the calibration procedure.

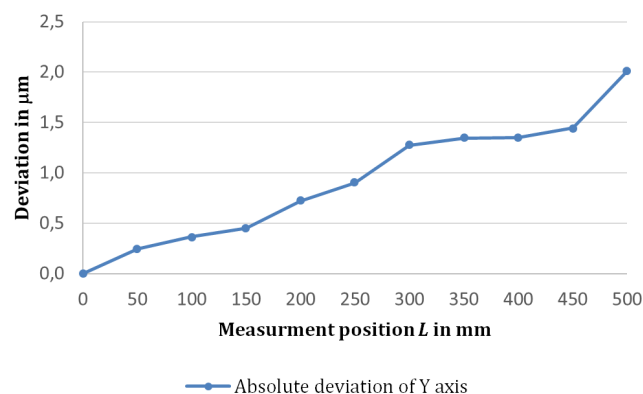


Fig. 5 Absolute deviation between laser values and encoder value

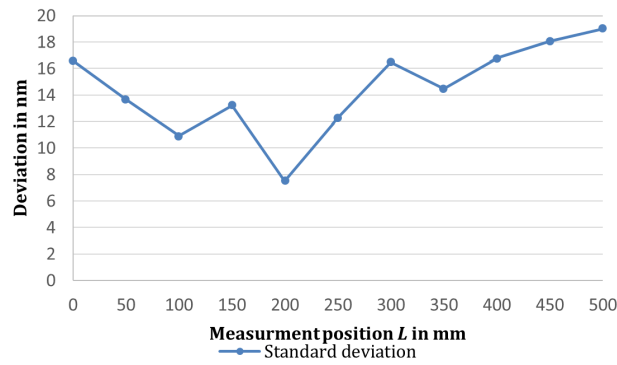


Fig. 6 Standard deviation on measurement positions

Measurement accuracy of the measuring system was verified on a calibrated line scale over the distance 0-100 mm. Experimental standard deviation $s(L)$ (12):

$$s(L) = \sqrt{\frac{1}{n-1} \sum_{j=1}^n (L_j - \bar{L})^2} \quad (12)$$

that reflects random influences is shown in the diagram in Fig. 7. The diagram also represents the deviation of measured values from the reference and estimated standard uncertainty. These results characterize the measuring system which will allow calibrations of length measurements without laser interferometer. Measuring results presented in Fig. 7 represent a linear characteristic. It is possible to compensate the error with the appropriate error mapping. From the results we can see that it is possible to improve the measurement uncertainty.

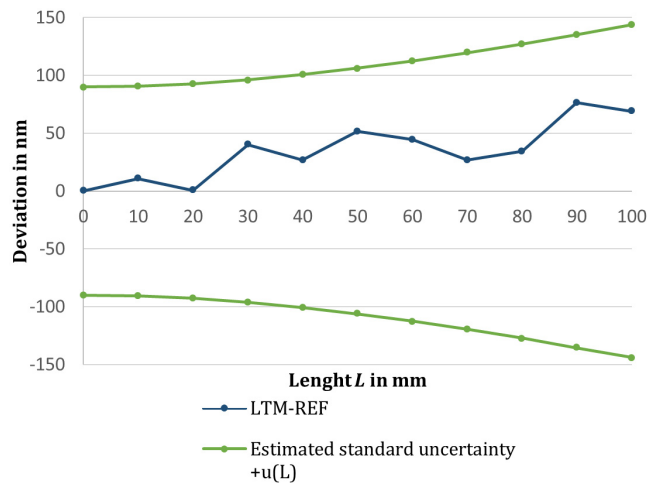


Fig. 7 Deviation of measured values from reference and estimated standard uncertainty

4. Conclusion

The main result of the presented research is a verified measuring set-up for calibrating line scales consisting of the numerical controlled multi-axis stage, the laser interferometer and the vision system for detecting line position.

The presented procedure for calibrating line-scales with lengths up to 500 mm, with the measuring uncertainty expressed by equation (11) has already been accredited by the national accreditation body. In respect to the previous measurement set-up, we have improved the measuring system with new automatic numerical controlled multi-axis stage, better CMOS

camera and better environmental conditions. Better calibration and measurement capability (CMC) was achieved and approved. Improved measuring set-up and system alignment [12] procedure lead to better Abbe error characterization. The calibration, verification and also error correction of optical CMMs is mainly based on measurements using reference line scales or two-dimensional grid plates [2]. Our further work will focus on calibrating 2D optical grids and evaluating uncertainty of this calibration. The validation process and verification procedure for measuring precise 2D grids is in preparation. One of the final goals of this validation phase was to determine uncertainty of measurement in calibration and verification of new automatic high resolution measuring set-up for calibrating precise line scales [13, 14].

Acknowledgement

The authors acknowledge the financial support from the Slovenian Research Agency (research core funding No. P2-0190), as well as from Metrology Institute of the Republic of Slovenia (funding of national standard of length; contract No. C3212-10-000072). The research was performed by using equipment financed from the European Structural and Investment funds (Measuring instrument for length measurement in two coordinates with sub-micrometer resolution; contract with MIRS No. C2132-13-000033).

References

- [1] Koops, R., Mares, A., Nieuwenkamp, J. (2010). A new standard for line-scale calibrations in the Netherlands, *Mikroniek – Professional Journal on Precision Engineering*, Vol. 50, No. 4, 5-12.
- [2] Meli, F. (2013). Calibration of photomasks for optical coordinate metrology, *Physikalisch-Technische Bundesanstalt (PTB)*, No. 8, 1-12, doi: [10.7795/810.20130620C](https://doi.org/10.7795/810.20130620C).
- [3] Kajima, M., Watanabe, T. Abe, M., Takatsuji, T. (2015). Calibrator for 2D grid plate using imaging coordinate measuring machine with laser interferometers, *International Journal of Automation Technology*, Vol. 9, No. 5, 541-545, doi: [10.20965/ijat.2015.p0541](https://doi.org/10.20965/ijat.2015.p0541).
- [4] Flügge, J., Köning, R., Weichert, Ch., Häßler-Grohne, W., Geckeler, R.D., Wiegmann, A., Schulz, M., Elster, C., Bosse, H. (2009). Development of a 1.5D reference comparator for position and straightness metrology on photomasks, In: *SPIE Proceedings, Photomask Technology 2008*, Vol. 7122, Monterey, CA, USA, doi: [10.1117/12.801251](https://doi.org/10.1117/12.801251).
- [5] Acko, B. (2012). Final report on EUROMET key comparison EUROMET.L-K7: Calibration of line scales, *Metrologia*, Vol. 49, doi: [10.1088/0026-1394/49/1A/04006](https://doi.org/10.1088/0026-1394/49/1A/04006).
- [6] Lassila, A. (2012). MIKES fibre-coupled differential dynamic line scale interferometer, *Measurement Science and Technology*, Vol. 23, No. 9, doi: [10.1088/0957-0233/23/9/094011](https://doi.org/10.1088/0957-0233/23/9/094011).
- [7] Leach, R. (2015). Abbe error/offset, In: Laperrière, L., Reinhart, G. (eds.), *CIRP Encyclopaedia of Production Engineering*, Springer, Berlin, Germany, 1-4, doi: [10.1007/978-3-642-35950-7_16793-1](https://doi.org/10.1007/978-3-642-35950-7_16793-1).
- [8] Klobucar, R., Acko, B. (2016). Experimental evaluation of ball bar standard thermal properties by simulating real shop floor conditions, *International Journal of Simulation Modelling*, Vol. 15, No. 3, 511-521, doi: [10.2507/ijimm15\(3\)10.356](https://doi.org/10.2507/ijimm15(3)10.356).
- [9] Družovec, M., Ačko, B., Godina, A., Welzer, T. (2009). Robust algorithm for determining line centre in video position measuring system, *Optics and Lasers in Engineering*, Vol. 47, No. 11, 1131-1138, doi: [10.1016/j.optlaseng.2009.06.017](https://doi.org/10.1016/j.optlaseng.2009.06.017).
- [10] Newport Corporation. Air bearing solution guide, from <https://www.newport.com/g/air-bearing-solution-selection-guide>, accessed December 2, 2016.
- [11] Köchert, P., Flügge, J., Köning, R., Weichert, C., Guan, J. (2013). Redetermination of the abbe errors' uncertainty contributions at the nanometer comparator, In: *Proceedings of the 9th International Conference on Measurement*, Smolenice, Slovakia, 171-174.
- [12] EA-4/02. Evaluation of the uncertainty of measurement in calibration, from <http://www.european-accreditation.org/publication/ea-4-02-m-rev01-september-2013>, accessed November 22, 2016.
- [13] Acko, B., Brezovnik, S., Crepinsek Lipus, L., Klobucar, R. (2015). Verification of statistical calculations in interlaboratory comparisons by simulating input datasets, *International Journal of Simulation Modelling*, Vol. 14, No. 2, 227-237, doi: [10.2507/IJSIMM14\(2\)4.288](https://doi.org/10.2507/IJSIMM14(2)4.288).
- [14] Acko, B., Sluban, B., Tasič, T., Brezovnik, S. (2014). Performance metrics for testing statistical calculations in interlaboratory comparisons, *Advances in Production Engineering & Management*, Vol. 9, No. 1, 44-52, doi: [10.14743/apem2014.1.175](https://doi.org/10.14743/apem2014.1.175).